

Photoionization of the hydrogen atom near the ionization limit in strong electric fields

H. Rottke and K. H. Welge

Fakultät für Physik, Universität Bielefeld, D-4800 Bielefeld 1, Federal Republic of Germany

(Received 14 February 1985)

The Stark spectroscopy of the hydrogen atom has been investigated near the ionization threshold in static homogeneous external electric fields from ~ 1000 to ~ 8000 V/cm with use of a two-step excitation $H(n=1) + \hbar\omega_{\text{vuv}} \rightarrow H(n=2) + \hbar\omega_{\text{uv}} \rightarrow H^*$ with vuv and uv laser radiation, independently tunable and linearly polarized either parallel (π) or perpendicular (σ) with respect to the external field. Different from other, nonhydrogenic atoms, the hydrogen atom is a peculiar case insofar as the initial states of $H(n=2)$, from which excitation takes place, are essentially of parabolic character at the field strengths employed in this study. Individual sublevels $(n_1, n_2, |m_l|)$ have been prepared in the $n=2$ state with sub-Doppler resolution. Photoionization spectra have been obtained with π - and σ -polarized uv radiation from the four possible sublevels of the $n=2$ Stark manifold: $|1,0,0\rangle |\pm \frac{1}{2}\rangle$, $|0,1,0\rangle |\pm \frac{1}{2}\rangle$, $|0,0,\pm 1\rangle |\pm \frac{1}{2}\rangle$, and $|0,0,\mp 1\rangle |\pm \frac{1}{2}\rangle$. All spectra show sharp line structures of quasistable field-ionizing states superimposed on continua in the energy region between the classical saddle point, $E_{\text{sp}} = -2\sqrt{F}$ a.u., and the zero-field ionization threshold $E=0$ a.u. Employing existing theoretical treatments, the quasistable spectral structures are quantitatively completely analyzed and accounted for, as long as their field ionization rate is less than $\sim 5 \times 10^{11} \text{ sec}^{-1}$. Field-ionization rates of quasistable states have been measured and are compared with theory. Oscillatory resonance structures of the ionization cross section near the zero-field threshold are observed with pronounced modulation degree only in the spectrum from the $|1,0,0\rangle |\pm \frac{1}{2}\rangle$ sublevel excited with the uv π -polarized. The energy spacing of the oscillations has been measured as a function of the electric field strength F and found to be nearly proportional to $F^{3/4}$, with slight but definite deviations. Theoretical analysis of the oscillations yields quantitative agreement with the experiment.

I. INTRODUCTION

The spectroscopy of atoms in high Rydberg states has gained considerable experimental and theoretical interest, particularly with the atoms excited around the ionization limit in strong external electric and magnetic fields.¹ While the extensive theoretical work in this field is largely based on the hydrogen atom, experimental studies have been performed almost exclusively with nonhydrogenic atoms, either because effects caused by nonhydrogenic interactions were to be studied or because of experimental difficulties encountered with hydrogen. In fact, no experiments are known with the H atom in strong magnetic fields with dominating diamagnetic interaction in high Rydberg states. In electric fields, Koch and collaborators²⁻⁶ performed investigations at excitation energies below the zero-field ionization limit, $E \leq 0$, and above the classical saddle-point energy $E_{\text{sp}} = -2\sqrt{F}$ a.u. (F being the electric field strength in atomic units). Using a fast-atomic-beam spectroscopy method combined with Stark tuning and fixed-frequency CO₂-laser excitation, they carried out precise measurements of the energy and the field-ionization rates of sharp quasistable states in that region and compared their experimental results with theory. Recently, Bergeman *et al.* reported laser-spectroscopy experiments on the Stark effect in the H atom in low states ($n \sim 4$) at very strong fields (3 MV/cm) in a high-energy beam (800 MeV).⁷

A conceptually straightforward and versatile method

widely used in laser-spectroscopy experiments with highly excited atoms is the state-selective excitation in thermal-energy atomic beams by a tunable laser combined with electric field ionization schemes.¹ Experimental obstacles that hindered the application of this technique to the hydrogen atom have been overcome by the development of the two-photon (vuv + uv) resonant excitation,

$$H(n=1) + \hbar\omega_{\text{vuv}} \rightarrow H(n=2) + \hbar\omega_{\text{uv}} \rightarrow H^*, \quad (1)$$

with the $n=2$ state as a resonant intermediate step, using independently tunable vuv and uv laser radiation.^{8,9} Experiments with this technique on the Stark effect of hydrogen in high Rydberg states have previously been reported including the observation of the cross-section oscillations in the continuum region above the zero-field ionization limit.⁹ Nayfeh and co-workers¹⁰ have done similar experiments with atomic hydrogen using, however, two-photon excitation of the $n=2$ state, with a third uv photon leading to excitation from $n=2$ to the Rydberg states.

The Stark effect of the hydrogen atom around the ionization threshold has been theoretically investigated quite extensively. The Schrödinger equation for the H atom in a homogeneous static electric field F is separable in parabolic coordinates.¹¹ Although the separated equations cannot be solved in closed analytic form, they can be integrated numerically to any degree of accuracy. Besides numerical treatments,¹²⁻¹⁴ Rayleigh-Schrödinger perturbation theory,^{5,15-17} and semiclassical procedures¹⁸⁻²³

have been employed to calculate positions of quasistable states in the ionization cross section in the classical field ionization region. The oscillatory structure in the cross section around the ionization threshold has also been thoroughly studied theoretically by several groups.^{13,20,22-25}

The objectives of this work have been the following. Firstly, a systematic study of the Stark spectroscopy of hydrogen atoms around the ionization threshold in homogeneous static electric fields from 1000 to 8000 V/cm, excited from selected Stark sublevels of the $n=2$ manifold to energies of H^* from the classical saddle point E_{SP} up into the continuum with $E \geq 0$. Secondly, investigation of the oscillatory structure of the ionization cross section in the region around the zero-field ionization limit. The oscillations in the ionization cross section around $E=0$ have previously been observed and investigated with nonhydrogenic atoms; Rb by Freeman *et al.*,^{26,27} Na by Metcalf *et al.*²⁸ and Ba and Na by Gallagher *et al.*²⁹ Thirdly, measurements of field-ionization rates of the quasistable states in the energy range $E_{SP} \leq E \leq 0$. Finally, discussion and analysis of the experimental results using existing theoretical approaches. An important additional aspect of the work is that it served as a preparing step for experiments with the H atom in strong magnetic fields.

II. EXPERIMENTAL

The central part of the experimental arrangement, the interaction region of the laser light with the hydrogen atoms, is schematically shown in Fig. 1. Hydrogen atoms are passed in a well-collimated beam through the electric field between two parallel-plate electrodes. The beam was intersected perpendicularly by the vuv and uv laser beams at the center of this arrangement, indicated in the figure by the solid circle. The atomic-beam divergence corresponded to a residual, perpendicular Doppler linewidth of ~ 2 GHz full width at half maximum (FWHM) at 121.6 nm. The laser beams counterpropagated in the interaction region, each having a diameter of ~ 2 mm at the intersection with the atomic beam. Electrons formed in the laser-atomic-beam interaction region were accelerated by the electric field, extracted through a fine mesh grid in the ground electrode, and detected by a secondary electron multiplier (SEM). Signals from the electron multiplier were amplified and recorded using a boxcar integrator.

Hydrogen atoms were obtained from a microwave discharge in hydrogen at 0.8 Torr pressure, and passed through a glass tube and capillary (1 mm diameter, 10 mm length) into the first differentially pumped section of the vacuum system. Recombination of the H atoms was prevented by coating the inner walls of the glass parts with phosphoric acid. The atomic beam was collimated by a skimmer and entered the second vacuum stage which was pumped cryogenically at a temperature of ~ 14 K by the metal housing shown in Fig. 1. Sheets attached to the housing (not shown in the figure) were coated with activated charcoal to specifically pump hydrogen at this temperature. The housing was provided with appropriate openings for the entrance and exit of the atomic and laser

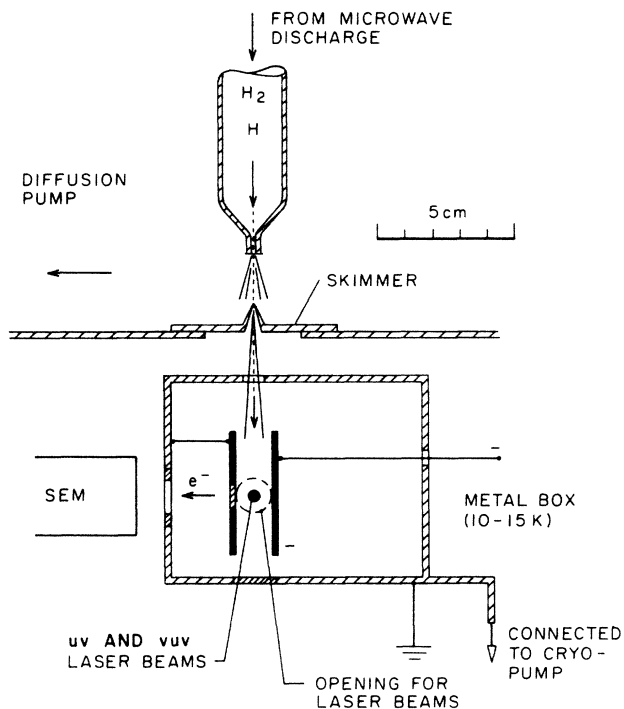


FIG. 1. Experimental arrangement, schematically.

beams, the electrons, and the high-voltage feedthrough. The interior of the metal box, acting as a third vacuum stage, was practically free of background gases. In this way photoionization of such gases by the laser radiation, otherwise leading to a background signal, was completely eliminated.

The tunable vuv radiation for the first excitation step at the Lyman- α wavelength (~ 121.6 nm) was generated by frequency tripling in krypton, $\omega_{vuv} = 3\omega_{uv}$. Different from a previously used procedure,³⁰ the fundamental, ω_{uv} , was obtained directly from an ultraviolet dye laser pumped by a XeCl excimer laser (308 nm). Typical working conditions and parameters of the uv radiation were ~ 14 mJ pulse energy, 10 ns pulse duration, ~ 0.9 GHz bandwidth, and 10 Hz pulse repetition rate, and for the vuv radiation $\sim 10^9$ photons/pulse and ~ 2.7 GHz bandwidth. Since the frequency of the fundamental radiation, ω_{uv} , matches within a fraction of a wave number the energy difference from the $H(n=2)$ state to the ionization limit, and since it had a rather high power, it can very efficiently photoionize the $H(n=2)$ atoms.³⁰ To avoid this, the uv radiation was spatially separated from the vuv by a monochromator arrangement with a 30° magnesium fluoride crystal prism between the tripling cell and the entrance to the vacuum chamber. The tunable ultraviolet for the second excitation step was obtained from a second dye laser. The tuning range of this uv radiation was 363.4–370.2 nm with a bandwidth $\Delta\nu_{uv} \sim 10$ GHz. Both dye lasers were pumped synchronously by the same excimer laser, so that the vuv and uv pulses arrived simultaneously at the intersection with the atomic beam.

The fine mesh grid in the ground field electrode for extraction of the electrons from the interaction region had a round transparent area of 0.5 cm diameter, which accord-

ingly defined an equally wide effective ionization-detection zone along the atomic beam. With an average speed of the H atoms of $\sim 2.7 \times 10^5$ cm/sec, this dimension determined the residence time of the atoms within the detection region of $\sim 2 \times 10^{-6}$ sec. This, in turn, resulted in a lowest observable limit for the electric field ionization rate of $\sim 5 \times 10^5$ sec $^{-1}$.

III. RESULTS

A. Stark splitting in H ($n=2$)

Since the excitation and ionization in electric fields depends essentially on the character of the states involved^{1(d),22} the level structure in the intermediate $n=2$ state had to be critically taken into account. Different from other atoms, e.g., alkali metals, the first excited state ($n=2$) of the hydrogen atom consists of two closely spaced s and p states, split only due to spin-orbit coupling and the Lamb shift. An external electric field, coupling the s with the p state, thus leads to a Stark effect which dominates the spin-orbit interaction in the $n=2$ manifold at rather low field strengths, as applied in these experiments. Figure 2(a) shows the Stark effect in $n=2$ as a function of the electric field strength with spin-orbit interaction and Lamb shift taken into account, as calculated by Lüders.³¹ Figure 2(b) shows, as an experi-

mental spectrum of the $n=1 \rightarrow n=2$ transition, taken at an electric field strength of 5460 V/cm with the vuv radiation parallel (π) and perpendicular (σ) polarized with respect to the electric field direction.

The $n=2$ Stark splitting was observed by scanning the vuv laser through the respective wavelength range while the uv radiation (from the second dye laser) was kept at a fixed wavelength. Because of the potential structure in the ionization cross section in the vicinity of the zero-field ionization limit, the uv wavelength was chosen such that the photon energy exceeded the zero-field limit by several hundred wave numbers, where the ionization spectrum is essentially structureless at the field strength applied.

The states in Fig. 2(a) are labeled in the low-field regime by the spherical quantum-number notation, indicating the fine-structure character from which they originate at $F=0$. In the high-field region they are labeled by the corresponding parabolic quantum-number notation, $|n_1, n_2, m_l\rangle |m_s\rangle$, with m_l and m_s the projections of the orbital and spin angular momenta onto the electric field direction, respectively.

At the fields employed in these experiments, the strong-field situation largely applies, which means that the states are of nearly pure parabolic character. Therefore, at $F=5460$ V/cm, the π and σ spectra in Fig. 2(b) should show, respectively, the inner and outer pairs of lines only. The low-intensity satellites should be substan-

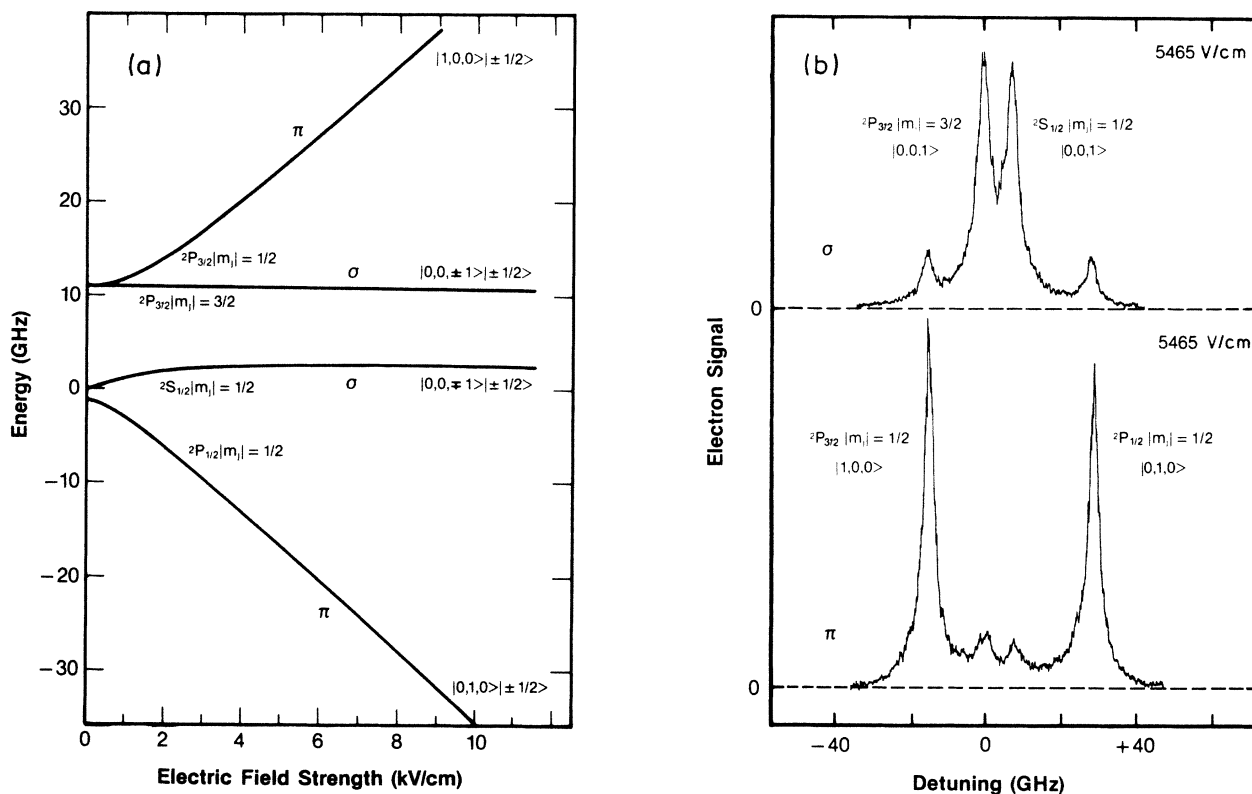


FIG. 2. (a) Calculated Stark splitting in the $n=2$ manifold as a function of the electric field strength F (Ref. 31). π and σ indicate, respectively, parallel and perpendicular polarization of the light necessary to excite the states in the high electric field limit. (b) Experimentally observed Stark splitting of the Lyman- α transition at $F=5460$ V/cm obtained at sub-Doppler resolution in an atomic beam using tunable vuv laser radiation. Polarization of the vuv radiation: σ (upper spectrum) and π (lower spectrum).

tially weaker than observed. Their appearance is rather caused by the vuv radiation not having been perfectly linearly polarized.

The purity of the character of a given substate with definite m_j in the $n=2$ manifold [i.e., ($|m_j| = \frac{3}{2}$) and ($|m_j| = \frac{1}{2}$) with $m_j = m_l + m_s$] is derived by expanding the total-state wave functions in parabolic state functions. For the states ($|m_j| = \frac{3}{2}$) this is simply

$$(|m_j| = \frac{3}{2}) = |0,0,\pm 1\rangle \pm |\pm \frac{1}{2}\rangle.$$

Thus the orbital part of the wave function consists of a pure parabolic function. For the other states the expansion yields

$$(|m_j| = \frac{1}{2}) = a_1 |1,0,0\rangle |\pm \frac{1}{2}\rangle + a_2 |0,1,0\rangle |\pm \frac{1}{2}\rangle + a_3 |0,0,\pm 1\rangle |\mp \frac{1}{2}\rangle.$$

For instance, for the uppermost of the four substates with $|m_j| = \frac{1}{2}$ correlating to ${}^2P_{3/2}$ $|m_j| = \frac{1}{2}$ one obtains at a field strength of 5714 V/cm, i.e., the field strength at which the spectra shown below have been taken, the following for the probability amplitudes: $a_1 = 0.979$, $a_2 = -0.092$, and $a_3 = -0.182$. With the square of the probability amplitudes as a quantitative measure of the character of a substate, this particular one has 96% $|1,0,0\rangle$ character at this field strength. The dependence of the squared amplitudes a_1^2 , a_2^2 , a_3^2 on the field strength

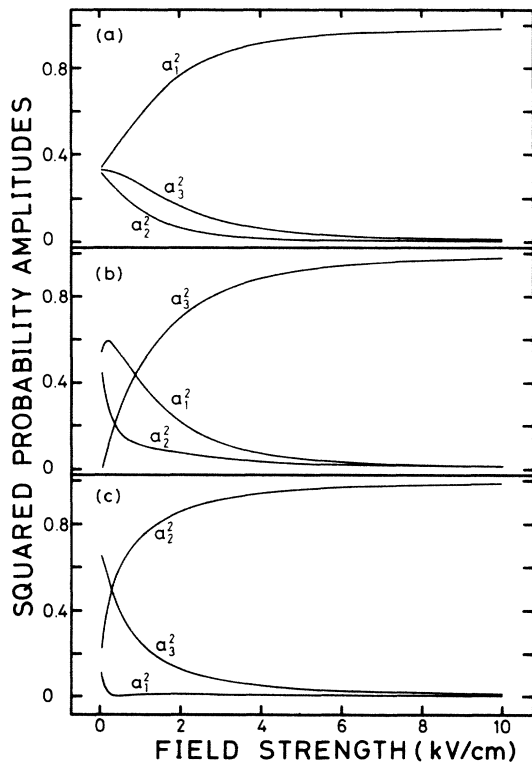


FIG. 3. Purity and character of the $n=2$ Stark states with $|m_j| = \frac{1}{2}$, represented by the squared probability amplitudes a_1^2, a_2^2, a_3^2 from the expansion in parabolic eigenfunctions (see text). (a) low-field state ${}^2P_{3/2}$, $|m_j| = \frac{1}{2}$, (b) low-field state ${}^2S_{1/2}$, $|m_j| = \frac{1}{2}$, (c) low-field state ${}^2P_{1/2}$, $|m_j| = \frac{1}{2}$.

is shown in Fig. 3 for the three possible ($m_j = \frac{1}{2}$) states. In these calculations it is assumed that the interaction of the atom with the external field does not yet mix the parabolic zero-field orbital wave function of the $n=2$ state with functions of states with different principal quantum number n , a valid assumption in the shown field-strength range.

B. Ionization spectra

Ionization spectra have been taken and investigated from all four of the $n=2$ substates with π and σ polarization of the uv ionizing light in an energy range from the classical saddle point, E_{SP} , up into the continuum region, $E \geq 0$. Examples, exhibiting all essential spectral features, are shown in Fig. 4, for an electric field strength $F = 5714$ V/cm. In taking the spectra the gain in the signal detection electronics was changed on five points in Figs. 4(b)–4(e) and 4(g). These points are indicated in the spectra and the corresponding changes in the gain are given. While taking a spectrum the uv intensity was monitored and the measured signal automatically normalized with respect to this intensity. The signal was not normalized with respect to the vuv intensity which was, however, monitored. Taking the changes in gain into account, the signal strengths can be compared in each spectrum to within a margin of $\pm 15\%$, given mostly by fluctuations and long-time drift of the average vuv intensity.

No ionization was detected in the classical tunnel region $E \leq E_{SP}$ because the field-ionization rate drops very quickly to below $5 \times 10^5 \text{ sec}^{-1}$,³² which is the lowest ionization rate observable in these experiments.

In the energy range $E_{SP} \leq E \leq 0$ all spectra exhibit sharp line structures of quasistable states superimposed on continua, whose intensities gradually increase starting at the classical saddle-point energy E_{SP} . The positions of these lines have been measured with an absolute accuracy of $\sim 0.8 \text{ cm}^{-1}$ and with a relative accuracy within a given spectrum of $\sim 0.1 \text{ cm}^{-1}$. Lines are labeled by the parabolic quantum numbers ($n_1, n_2, |m_l|$) of the respective final ionizing states, grouped together in sets according to their principal quantum numbers given by the relation $n = n_1 + n_2 + |m_l| + 1$. The identification and assignment of the lines has been achieved by calculating the energy of the corresponding quasistable states, as discussed below.

In addition to the assigned lines, which should appear due to the intermediate state and polarization direction of the ionization laser beam chosen, the spectra contain lines with relatively lower intensity. Their appearance has two possible causes. Firstly, the dominant contribution to their appearance is due to the imperfect π or σ linear polarization of the uv radiation. Secondly, the intermediate $n=2$ substate does not have a 100% pure parabolic state character, but contains small admixtures from other parabolic substates; that is, more than one of the a_i in the expansion of the intermediate state in parabolic states is different from zero. These lines have been identified and are found as "strong" lines in one of the other spectra, therefore, they are not labeled.

If one corrects for the gain of the detection electronics, Figs. 4(c) and 4(e) and Figs. 4(d) and 4(f) resemble each

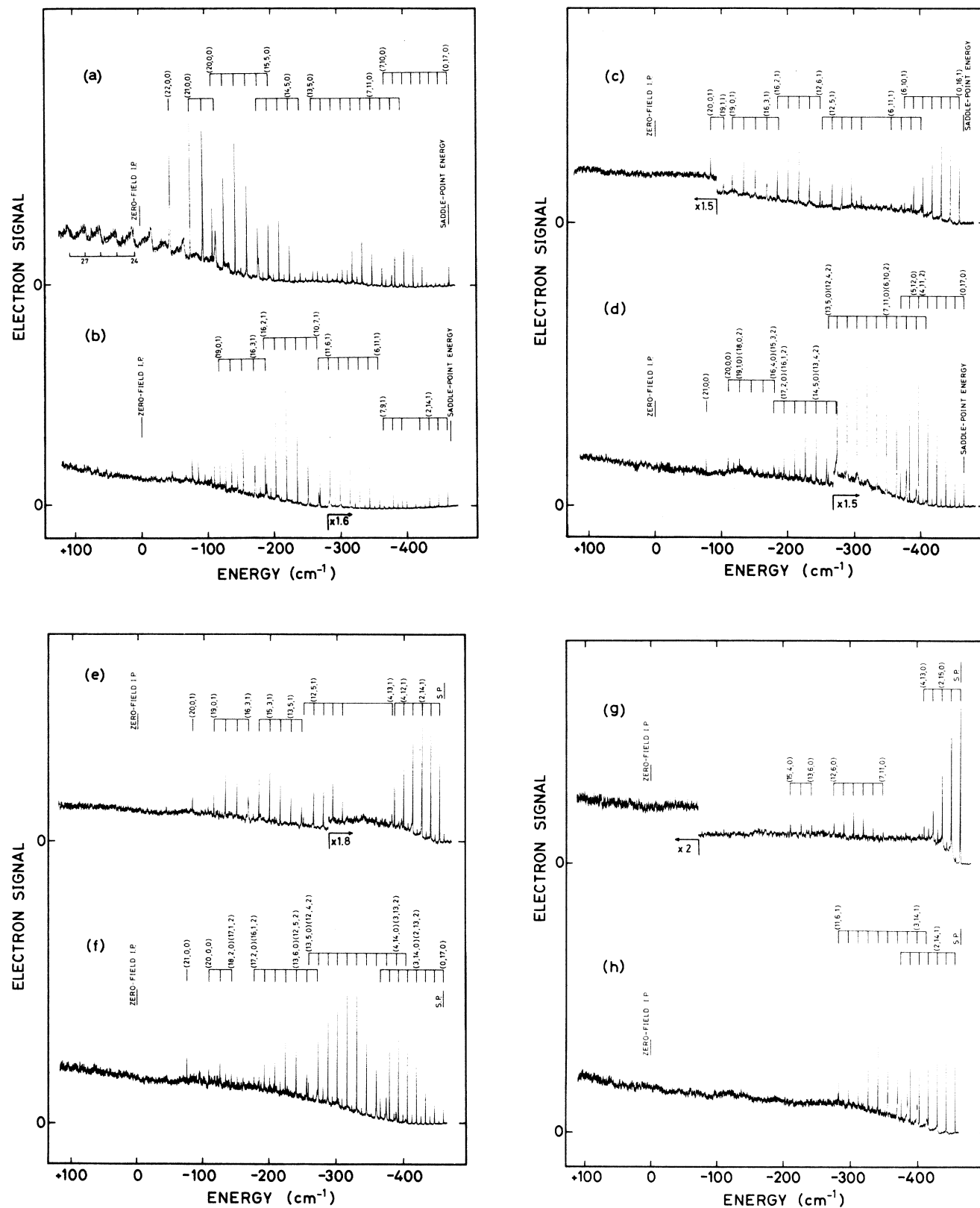


FIG. 4. Photoionization spectra excited from individual Stark sublevels in the $n=2$ manifold in an electric field $F=5714$ V/cm with π - and σ -polarized uv radiation. Indicating the four $n=2$ states by the high-field parabolic quantum-number notation and the excitation from these states by the polarization of the ionizing light, the eight spectra are labeled, respectively, (a) $|1,0,0\rangle | \pm \frac{1}{2} \rangle -\pi$; (b) $|1,0,0\rangle | \pm \frac{1}{2} \rangle -\sigma$; (c) $|0,0,\pm 1\rangle | \pm \frac{1}{2} \rangle -\pi$; (d) $|0,0,\pm 1\rangle | \pm \frac{1}{2} \rangle -\sigma$; (e) $|0,0,\mp 1\rangle | \pm \frac{1}{2} \rangle -\pi$; (f) $|0,0,\mp 1\rangle | \pm \frac{1}{2} \rangle -\sigma$; (g) $|0,1,0\rangle | \pm \frac{1}{2} \rangle -\pi$; (h) $|0,1,0\rangle | \pm \frac{1}{2} \rangle -\sigma$.

other closely with respect to the heights of the quasistable states below the zero-field ionization threshold. This is due to the fact that at the field strength of 5714 V/cm the intermediate $n=2$ state in Figs. 4(c) and 4(d) is the pure parabolic state $|0,0,\pm 1\rangle$ and in spectra 4(e) and 4(f) it is nearly the pure $|0,0,\pm 1\rangle$ parabolic state, as can be seen from the plot of the a_i^2 in Fig. 3(b).

A direct comparison of the observed quasistable-state line heights in our spectra with theoretically calculated ionization cross sections at the position of the resonances is not possible for two reasons. Firstly, the measured line heights depend on the relative magnitude of the true resonance width and the uv ionization laser bandwidth. Secondly, due to the finite residence time of the highly excited atoms in the detection volume and the pulsed electron-detection technique, only electrons arriving at the multiplier during a certain time interval after the excitation laser pulse could be detected in this experiment. This causes discrimination of signal intensities of quasistable states according to their various ionization rates. For instance, states with lifetimes longer than about 2×10^{-6} sec are not observed (see above).

The spectrum in Fig. 4(a) exhibits the sought-for oscillatory structure, extending from below the zero-field ionization threshold well into the continuum region $E \geq 0$. The degree of modulation, defined by $2(S_{\max} - S_{\min}) / (S_{\max} + S_{\min})$, where S_{\max} and S_{\min} are the signal heights at adjacent maxima and minima, is $39 \pm 5\%$ for the oscillation next to the zero-field ionization threshold. No oscillations were detectable in any of the other spectra at the field strengths of this work. Taking the precision limit of the present measurements into account, the modulation degree was less than a few percent in these cases.

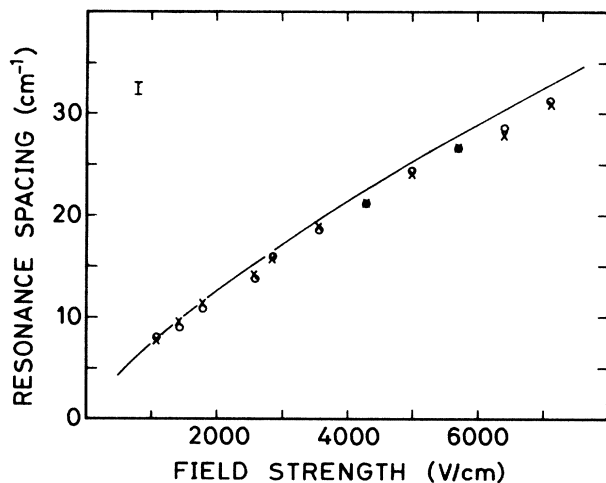


FIG. 5. Energy spacing of the oscillations in the ionization spectrum from the $|1,0,0\rangle |\pm \frac{1}{2}\rangle$ state with π -polarized uv light as a function of the electric field strength. The spacing refers to the distance of the first two adjacent maxima above the zero-field ionization threshold, $E=0$. Open circles, measured values; solid line, theoretical $F^{3/4}$ dependence; crosses, theoretical results as discussed in the text. Vertical bar indicates the experimental error limit.

C. Field-strength dependence of the oscillation spacing

According to theory^{20,24,25} and previous measurements with Rb (Refs. 26 and 27) and Na (Refs. 28 and 29) the spacing of adjacent oscillation maxima (or minima) has a field-strength dependence proportional to $F^{3/4}$ at $E=0$. Figure 5 shows measurements (open circles) at field strengths between 1000 V/cm and 7000 V/cm with π -polarized uv radiation from the $|1,0,0\rangle$ intermediate state. The measured points, with the margin of error given by the vertical bar in the figure, lie systematically slightly below the theoretical $F^{3/4}$ curve (solid line). Better agreement exists with results of a calculation which will be discussed below (crosses in Fig. 5).

D. Quasistable-state field-ionization rates

The field-ionization rate of the quasistable states in the energy range $E_{\text{SP}} \leq E \leq 0$ can be obtained in experiments of the present kind in two complementary ways: (a) signal decay measurements as a function of the time after the pulsed excitation and (b) linewidth measurement. Rather than to perform detailed and systematic measurements, the main objective in this work was to demonstrate the feasibility of both methods.

The signal decay method can be employed in the decay-rate range given by $1/t_r \leq R_{\text{ion}} \leq 1/t_l$, where t_l is the laser pulse duration and t_r is the residence time of the excited atoms in the effective ionization-detection region (see above). With $t_l \sim 10^{-8}$ sec and $t_r \sim 2 \times 10^{-6}$ sec in this work we obtain $5 \times 10^5 \leq R_{\text{ion}} \leq 10^8$ sec⁻¹. Figure 6 shows results of measurements carried out at $F=5714$ V/cm for some substates in the $n=18$ and 19 manifolds. The rates have been derived in a straightforward manner

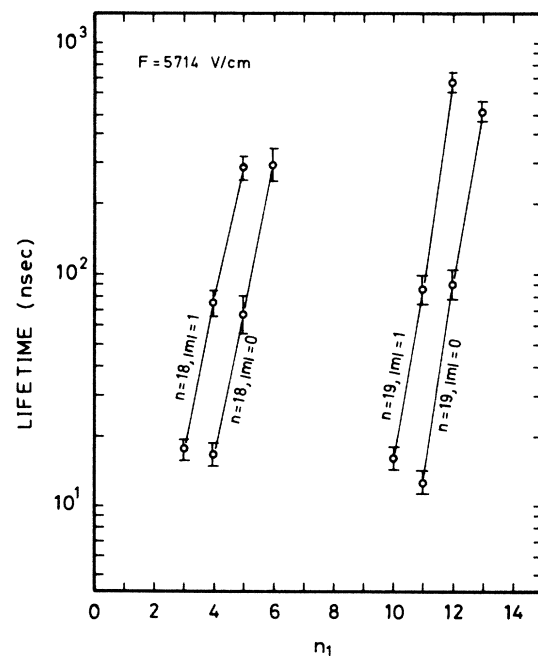


FIG. 6. Electric field ionization lifetime of quasistable states in the $n=18$ and 19 final-state manifolds measured at $F=5714$ V/cm.

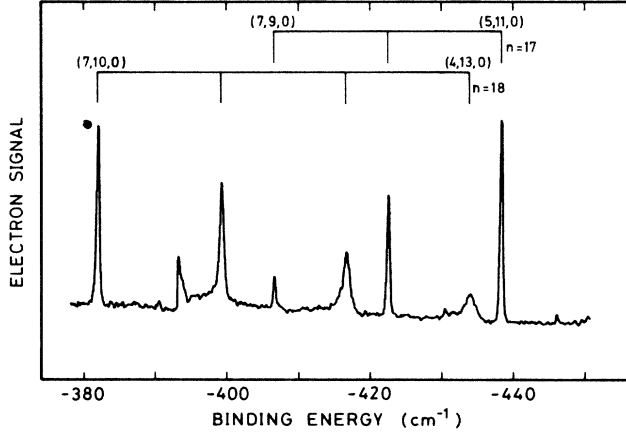


FIG. 7. Section of an ionization spectrum showing the field-ionization lifetime through linewidth broadening. The intermediate state is $|1,0,0\rangle|\pm\frac{1}{2}\rangle$; the ionizing radiation is π -polarized and the field strength 7140 V/cm.

from the observed exponential signal time dependence: $S(t)/S(t=0) = \exp(-t/\tau_{\text{ion}})$ where $S(t)$ and $S(t=0)$ are the signals at time t and $t=0$, respectively. The general lifetime behavior observed is (a) exponential increase with the quantum number n_1 within a given n -manifold and for a given m_l and (b) decrease with increasing principal quantum number n .

The decay-rate range in which the linewidth method can be used, depends of course on the spectral resolution $\Delta\nu_{\text{res}}$ according to $R_{\text{ion}} = 1/\tau_{\text{ion}} \geq 2\pi\Delta\nu_{\text{res}}$, where $\Delta\nu_{\text{res}}$ is the total resolution in the ionizing step determined by the Doppler width and the laser bandwidth. In these experiments the Doppler width was negligibly small compared to the uv laser bandwidth of ~ 10 GHz so that $R_{\text{ion}} \geq 6 \times 10^{10} \text{ sec}^{-1}$. Figure 7 shows, as an example, a section of the spectrum excited from the state $|1,0,0\rangle$ to final states in the $n=17$ and 18 manifolds with π -polarized uv light at a field strength $F=7140$ V/cm. Taking for instance the line (5,12,0), its half-width of 1.1 cm^{-1} corresponds to a lifetime of the upper state of ~ 5 ps due to electric field ionization. Comparison with the results of the direct decay measurements shows qualitatively the same dependence on the state quantum numbers.

A comparison of the experimental results given in Fig. 6 with values calculated from an asymptotic relation for the field-ionization rate given by Damburg and Kolosov³² shows for the $n=18$ states discrepancies of up to a factor of 3 and for the (10,7,1) state in the $n=19$ manifold of even a factor of ~ 18 . This finding is in agreement with measurements of Koch *et al.*,⁴ who also found discrepancies of up to a factor of 10 of their results compared to this asymptotic relation.

IV. DISCUSSION

A. Quasistable states

The nonrelativistic theory of the H atom in electric fields has been advanced to a point such that line posi-

tions of the quasistable-state spectra in the energy range $E \leq 0$ can be calculated to virtually any desired degree of accuracy. Following a perturbation procedure previously developed and employed by Silverstone,^{15,16} Silverstone and Koch,⁵ and Damburg and Kolosov,¹⁷ we have calculated the energies of the final states $|n_1, n_2, |m_l\rangle\rangle$ to a degree of accuracy better than that of our experimental absolute ($\sim 0.8 \text{ cm}^{-1}$) and relative ($\sim 0.1 \text{ cm}^{-1}$) line-position measurement. In this way the identification of the lines with the corresponding final-state parabolic quantum numbers was possible. The procedure starts from the Schrödinger equation for the H atom in an electric field F ,

$$\left[-\frac{\Delta}{2} - \frac{1}{r} + Fz \right] \psi = E\psi, \quad (2)$$

separated in parabolic coordinates,

$$\frac{d^2\chi_1}{d\xi^2} + \left[\frac{E}{2} - \frac{m_l^2 - 1}{4\xi^2} + \frac{Z_1}{\xi} - \frac{F}{4}\xi \right] \chi_1 = 0, \quad (3a)$$

$$\frac{d^2\chi_2}{d\eta^2} + \left[\frac{E}{2} - \frac{m_l^2 - 1}{4\eta^2} + \frac{Z_2}{\eta} + \frac{F}{4}\eta \right] \chi_2 = 0, \quad (3b)$$

where the ansatz

$$\psi = (2\pi\xi\eta)^{-1/2} e^{im_l\phi} \chi_1(\xi)\chi_2(\eta) \quad (4)$$

was used with the separation constants Z_1, Z_2 related to each other through $Z_1 + Z_2 = 1$.

Starting with the zero-field ($F=0$) wave functions and values for the separation constants Z_1, Z_2 , given by

$$Z_i = (-2E)^{1/2} [n_i + (|m_l| + 1)/2] \quad (i=1,2),$$

the Rayleigh-Schrödinger perturbation series for Z_1 and Z_2 is calculated up to an order $2N$, where N can be an arbitrary positive integer:

$$Z_i^{(2N)}(n_i, |m_l|, E, F) = \sum_{k=0}^{2N} a_k^{(i)}(n_i, |m_l|, E) F^k \quad (i=1,2). \quad (5)$$

Subsequently, the diagonal Padé approximants $[N/N]$ of order N to these series are determined using the following relation for the general Padé approximant $[L/M]$:^{5,33}

$$\begin{aligned} & [L/(M+1)] \\ &= [L/M] + \{ [(L+1)/M] - [L/M] \}^{-1} \\ & \quad + \{ [(L-1)/M] - [L/M] \}^{-1} \\ & \quad - \{ [L/(M-1)] - [L/M] \}^{-1} \}^{-1} \quad (6) \end{aligned}$$

starting with $[L/0] = Z_i^{(L)}(n_i, |m_l|, E, F)$ ($i=1,2$). The state energies $E_{n_1, n_2, |m_l|}(F)$ are then obtained from the coupling relation $Z_1 + Z_2 = 1$.

The $[12/12]$ diagonal Padé approximant to the separation constants was usually sufficient to calculate $E_{n_1, n_2, |m_l|}(F)$ to an accuracy which agreed with the observed line positions of the quasistable states to within experimental accuracy as long as the field-ionization rate

R_{ion} of the states, derived from the asymptotic formula given by Damburg and Kolosov,³² was smaller than $\sim 5 \times 10^{11} \text{ sec}^{-1}$. For $R_{\text{ion}} \geq 5 \times 10^{11} \text{ sec}^{-1}$ the above method for calculation of the quasistable-state positions yielded values no longer in agreement with experiment.

B. Continuum oscillations

The oscillations in the continuum ionization cross section for $E > 0$ have been thoroughly investigated theoretically in recent years using the Wentzel-Kramers-Brillouin (WKB) method²⁰⁻²⁵ and also using numerical integration of the Schrödinger equation.¹³ The occurrence of the oscillations in the spectrum with π -polarized excitation from the $|1,0,0\rangle$ state [Fig. 4(a)] can be quantitatively completely accounted for following the WKB procedures of Kondratovich and Ostrovsky²³ and Harmin^{21,22} to derive approximate solutions of the equations of motion [Eqs. 3(a) and 3(b)]. The ionization cross section $\sigma_{(n_1, n_2, |m_l|)}^p(E)$, with $p = \pi, \sigma$ indicating the polarization of the light relative to the electric field, can be written as a sum over partial cross sections for ionization into final continuum states $|E, F, n_1^f, m_1^f\rangle$ with definite parabolic quantum number n_1^f :^{20,21}

$$\sigma_{(n_1, n_2, |m_l|)}^p(E) = \sum_{n_1^f=0}^{\infty} \sigma_{(n_1, n_2, |m_l|)}^p(E, n_1^f). \quad (7)$$

The initial state from which the excitation takes place, here a Stark level in $n=2$, is given by a zeroth-order parabolic Coulomb wave function with quantum numbers n_1, n_2, m_l . This approximation for the strongly bound initial level in $n=2$ is correct for the electric field strengths used in these experiments. Each one of the partial cross sections is given by²¹

$$\sigma_{(n_1, n_2, |m_l|)}^p(E, n_1^f) = 4\pi^2 \alpha \hbar \omega |\langle E, F, n_1^f, m_1^f | O | n_1, n_2, m_l \rangle|^2 \quad (8)$$

with $O=z$ for π -polarized and $O=x$ for σ -polarized light of frequency ω , the z axis being the electric field direction. In the range where the initial-state wave functions $|n_1, n_2, m_l\rangle$ are substantially different from zero, which is close to the proton, the interaction with the external electric field is small compared to the Coulomb electron-proton interaction, even for the atom in the final state $|E, F, n_1^f, m_1^f\rangle$. In the calculation of the matrix element (8) one thus may use hydrogenic wave functions for the final states:^{20,23}

$$|E, F, n_1^f, m_1^f\rangle = (2\pi\xi\eta)^{-1/2} e^{im_1^f\varphi} \chi_1(\xi)\chi_2(\eta). \quad (4')$$

The functions $\chi_j(x)$ are given by

$$\chi_j(x) = A_j x^{(m_1^f+1)/2} e^{-ikx/2} \times {}_1F_1 \left[i \frac{Z_j}{k} + \frac{m_1^f+1}{2}; m_1^f+1; ikx \right], \quad (9)$$

where $j=1,2$, $x=\xi, \eta$, and $k=(2E)^{1/2}$ for $E \geq 0$, $k=i(-2E)^{1/2}$ for $E \leq 0$, and the Z_j are the separation constants. ${}_1F_1$ is the confluent hypergeometric function

and $A_j(E, F, n_1^f, m_1^f)$ are the normalization constants for $\chi_j(x)$. The constants A_j ($j=1,2$) depend on the long-range behavior of the wave function $|E, F, n_1^f, m_1^f\rangle$ and, therefore, strongly on the electric field F . Using the initial parabolic states $|1,0,0\rangle$, $|0,1,0\rangle$, and $|0,0,1\rangle$ relevant in this experiment, analytic formulas for the partial cross sections (8) are calculated using the approximations given above. With the abbreviation

$$N(E, F, n_1^f, m_1^f) = |A_1(E, F, n_1^f, m_1^f) A_2(E, F, n_1^f, m_1^f)|^2$$

one obtains

$$\sigma_{(1,0,0)}^{\pi}(E, n_1^f) = 4f(E)N(E, F, n_1^f, 0) \times \left[Z_1^2 - \frac{3}{4}Z_1 + k^2Z_1 - \frac{k^2}{2} + \frac{1}{16} \right]^2, \quad (10)$$

$$\sigma_{(1,0,0)}^{\sigma}(E, n_1^f) = 2f(E)N(E, F, n_1^f, 1)(Z_1 + k^2 - \frac{1}{4})^2, \quad (11)$$

$$\sigma_{(0,0,1)}^{\pi}(E, n_1^f) = f(E)N(E, F, n_1^f, 1)(Z_2 - Z_1)^2, \quad (12)$$

$$\sigma_{(0,0,1)}^{\sigma}(E, n_1^f) = f(E) \left[16N(E, F, n_1^f, 2) + \frac{9}{4}N(E, F, n_1^f, 0) \times \left[Z_1Z_2 + \frac{k^2}{4} - \frac{1}{8} \right]^2 \right]. \quad (13)$$

The corresponding cross sections for the state $|0,1,0\rangle$ can be derived from Eqs. (10) and (11) by simply replacing Z_1 by $Z_2 = 1 - Z_1$ in the last factors. The factor $f(E)$, being independent of n_1 and F , is a slowly varying function of the energy:

$$f(E) = 2^{18} \pi^2 \alpha \frac{1}{(1+4k^2)^7} \left| \left[\frac{1+2ik}{1-2ik} \right]^{i/k} \right|^2. \quad (14)$$

It essentially represents the energy dependence of the zero-field photoionization cross section of the hydrogen atom from the initial state $n=2$ in the energy region $E \geq 0$. The factor N , called partial density of final states by Luc-Koenig and Bachelier,¹³ is substantially different from zero only in the range $0 \leq Z_1 \leq 1$. Outside this region it drops to zero exponentially in the energy, except at the resonances of the quasistable states in the range $E \leq 0$.^{13,21} Figure 8(a) shows N as a function of the energy in the range $E \geq 0$ and its dependence on the quantum number n_1 for $m_l=0$ at a field strength $F=5714 \text{ V/cm}$, employed in the experimental spectra (Fig.4). The arrows in Fig. 8 indicate the positions $Z_1=0$ and 1. The analytic expressions for the normalization constants A_1, A_2 were derived using the WKB approximation method of Kondratovich and Ostrovsky.²³ Because N varies only slowly with the energy in the range $0 \leq Z_1 \leq 1$ the partial density of states alone obviously cannot account for the oscillations of the total ionization cross section observed in the spectrum of Fig. 4(a).

The partial ionization cross section for the initial states $|1,0,0\rangle$ and $|0,1,0\rangle$ with π -polarized light calculated for $n_1=26$ from relation (10) is shown in Fig. 8(b). Comparison of Figures 8(a) and 8(b) shows that the structure in the partial cross sections $\sigma_{(1,0,0)}^{\pi}(E, n_1^f)$ (curve I) and $\sigma_{(0,1,0)}^{\pi}(E, n_1^f)$ (curve II) between $Z_1=0$ and 1 is deter-

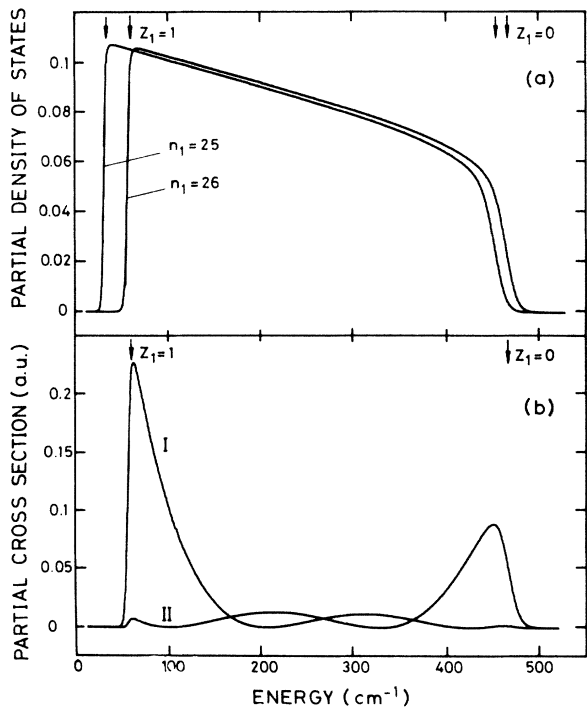


FIG. 8. (a) Calculated density of states N above the zero-field ionization threshold for final states with quantum numbers $n_1=25, 26$ at $F=5714$ V/cm. Positions $Z_1=0$ and 1 are indicated by the arrows. (b) Calculated partial photoionization cross sections for excitation from the parabolic states $|1,0,0\rangle$ and $|0,1,0\rangle$ into the channel with quantum number $n_1=26$ at 5714 V/cm in the energy region $E \geq 0$. Curve I, partial cross section $\sigma_{\pi_{1,0,0}}^{\pi}(E, n_1)$; curve II, partial cross section $\sigma_{\pi_{0,1,0}}^{\pi}(E, n_1)$.

mined essentially by the last factor in relation (10), namely,

$$(Z_1^2 - 3Z_1/4 + k^2Z_1 - k^2/2 + \frac{1}{16})^2$$

for $\sigma_{\pi_{1,0,0}}^{\pi}(E, n_1^f)$ and the corresponding relation for $\sigma_{\pi_{0,1,0}}^{\pi}(E, n_1^f)$, with Z_1 replaced by $Z_2 = 1 - Z_1$.

The partial cross section $\sigma_{\pi_{1,0,0}}^{\pi}(E, n_1^f)$ shows a pronounced, relatively narrow maximum near $Z_1 \sim 1$ with the cross section in the remaining energy range being about a factor of 20 smaller. This maximum near $Z_1 \sim 1$ is responsible for the oscillations in the photoionization cross section of the state $|1,0,0\rangle$ with π -polarized light near the zero-field ionization threshold, as will be shown below. The analogous maximum that appears near $Z_1 \sim 0$ in $\sigma_{\pi_{0,1,0}}^{\pi}(E, n_1^f)$ [curve II in Fig. 8(b)], is seen to be smaller and broader than the one in $\sigma_{\pi_{1,0,0}}^{\pi}(E, n_1^f)$, resulting in much smaller oscillation amplitudes in the total cross section, consistent with the experimental results. As can be seen in Fig. 8(a), the flattening of the maximum in $\sigma_{\pi_{0,1,0}}^{\pi}(E, n_1^f)$ is due to the much more smooth decrease to zero in the partial density of states N near $Z_1 \sim 0$.

As discussed above, the maximum of the cross-section oscillations for $E \geq 0$ in the photoionization cross section of $|1,0,0\rangle$ with π -polarized light should appear at $Z_1 \sim 1$. Using this result the approximate positions of the maxima can simply be calculated by means of the WKB quantization condition for the bound motion along the ξ

coordinate direction:

$$\int_{\xi'}^{\xi''} q(\xi) d\xi = (n_1 + \frac{1}{2})\pi, \quad (15)$$

with the WKB wave number

$$q(\xi) = \left[\frac{E}{2} - \frac{m_l^2}{4\xi^2} + \frac{Z_1}{\xi} - \frac{F}{4}\xi \right]^{1/2} \quad (16)$$

from the equation of motion (3a) incorporating the Langer correction.²¹ ξ' and ξ'' are the positive zeros of $q(\xi)$. Setting now $m_l=0$ and $Z_1=1$ in the expression for $q(\xi)$ yields the approximate position of the oscillation maxima. The result for $F=5714$ V/cm is shown in the experimental spectrum [Fig. 4(a)], where maxima positions above $E=0$, calculated from (15), for $n_1=24-28$ are indicated by marks. The agreement with the observed positions of the maxima is seen to be quite good.

The energy spacing ΔE between adjacent resonance maxima at $E=0$ is approximately given by the derivative dE/dn_1 ($E=0$) calculated by differentiating the WKB quantization condition (15) with respect to n_1 .^{20,24,25} The result is

$$\Delta E = 2\pi^{1/2} \frac{\Gamma(\frac{1}{4})}{\Gamma(\frac{3}{4})} \left[\frac{F}{4} \right]^{3/4}. \quad (17)$$

The larger the parabolic quantum number n_1 for the resonance at $E=0$, the better this $F^{3/4}$ field-strength dependence should approximate the actual resonance spacing. This behavior can be seen in Fig. 5. The $F^{3/4}$ dependence plotted in Fig. 5 as the solid line represents the experimental results (open circles) more closely at lower field strengths than at high field strengths, in agreement with

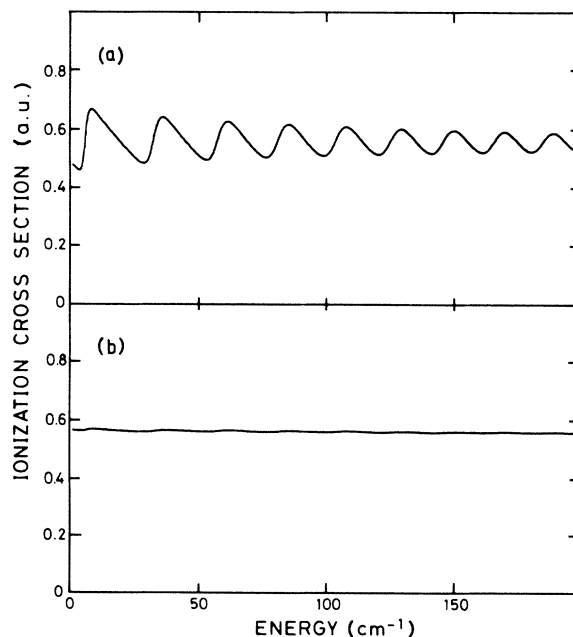


FIG. 9. Calculated total photoionization cross sections for π -polarized excitation from the parabolic states $|1,0,0\rangle$ and $|0,1,0\rangle$ at 5714 V/cm. (a) Cross section $\sigma_{\pi_{1,0,0}}^{\pi}(E)$; (b) cross section $\sigma_{\pi_{0,1,0}}^{\pi}(E)$.

the fact that the n_1 quantum number of the resonance at threshold increases with decreasing electric field strength. Closer agreement over the whole investigated field-strength range with the measured resonance spacings is obtained, if instead of the approximate relation (17), the WKB quantization condition (15) is directly used to calculate the positions of the first two maxima above $E=0$. The results thus obtained are shown as crosses in Fig. 5.

Figures 9(a) and 9(b) show the total ionization cross sections $\sigma_{(1,0,0)}^\pi(E)$ and $\sigma_{(0,1,0)}^\pi(E)$ obtained by summing up the corresponding partial cross sections in the energy range $E \geq 0$ for an electric field strength of 5714 V/cm. While $\sigma_{(0,1,0)}^\pi(E)$ is virtually flat, $\sigma_{(1,0,0)}^\pi(E)$ is modulated strongly with 36.8% at $E=0$, which agrees well with the experimental result of $39 \pm 5\%$.

The experimentally observed decrease of the modulation degree with increasing energy is due to a decrease of the height of the maxima in the partial cross sections $\sigma_{(1,0,0)}^\pi(E, n_1')$ with increasing n_1 . Also, the oscillations are getting more symmetric at higher energy because the increase of $\sigma_{(1,0,0)}^\pi(E, n_1')$ from zero at $Z_1 \geq 1$ to the maximum at $Z_1 \sim 1$ is less steep for higher values of the quantum number n_1 .

Different from $\sigma_{(1,0,0)}^\pi(E)$, the cross section for photoionization from the $|0,1,0\rangle$ state by π -polarized light, $\sigma_{(0,1,0)}^\pi(E)$ hardly shows any oscillations above $E=0$ [Fig. 9(b)] in agreement with the experiment [Fig. 4(g)]. The broad flat maxima in the theoretical partial cross sections $\sigma_{(0,1,0)}^\pi(E, n_1')$ [Fig. 8(b), curve II] near $Z_1 \sim 0$ cause the oscillations to have a very small modulation depth, which is calculated to be 1.16%. Similar small oscillations result from the calculation of the photoionization cross section from the state $|0,0,1\rangle$ and for all intermediate states ionized with σ -polarized radiation. As far as the cross-section oscillations above the zero-field-ionization threshold are concerned the relatively simple theoretical WKB approximation, which gives analytical relations for the cross sections, can completely account for our experimental results. It was not necessary to employ tedious numerical integration procedures to solve the equations of

motion (3).

The time-dependent wave-packet approach, as put forward by Reinhardt,³⁴ provides another physical model to visualize the oscillatory structures and to explain them in a semiclassical time-dependent wave-packet treatment. In this model excitation, for instance, from the $|1,0,0\rangle$ state, oriented in the upward field direction, with π -polarized light results in an equally localized initial wave packet moving along the z -axis up the field, being reflected back to the ion core with some recurrence time. This quasiperiodic kind of wave-packet motion in the time domain in turn correlates with the oscillatory energy dependence of the ionization cross section. On the other hand, excitation from the $|0,1,0\rangle$ state, again with π -polarized light, produces the initial wave packet also oriented along the z axis, but in the down-field direction. This results in a corresponding initial motion of the packet in the ionizing direction essentially with much lower recurrence amplitude. Because of the weak reflection the oscillation amplitudes are correspondingly small in this situation.

V. CONCLUSIONS

In this work the photoionization of the hydrogen atom in a strong external electric field has been systematically studied by state-selective excitation from all four Stark sublevels in the $H(n=2)$ state manifold, using two-step excitation by tunable vuv + uv laser radiation. The eight possible types of ionization spectra excited with parallel (π) and perpendicular (σ) linearly polarized vuv and uv radiation in both steps show structures of quasistable field-ionizing states and oscillatory resonances in the ionization cross section. All observed spectral features can be quantitatively completely accounted for by existing theories, as was to be expected. This work has also indicated the feasibility of analogous experiments with the H atom excited around the ionization threshold in strong magnetic and crossed magnetic-electric fields, now in progress in our laboratory.

¹(a) See J. Phys. (Paris) Colloq. **43**, C2 (1982); (b) S. Feneuille and P. Jacquinet, Adv. At. Mol. Phys. **17**, 99 (1981); (c) *Rydberg States of Atoms and Molecules*, edited by R. F. Stebbings and F. B. Dunning (Cambridge University, Cambridge, 1983); (d) C. W. Clark, K. T. Lu, and A. F. Starace, in *Progress in Atomic Spectroscopy*, edited by H. J. Beyer and H. Kleinpoppen (Plenum, New York, 1984), Part C.

²P. M. Koch, Phys. Rev. Lett. **41**, 99 (1978).

³P. M. Koch and D. R. Mariani, J. Phys. B **13**, L645 (1980).

⁴P. M. Koch and D. R. Mariani, Phys. Rev. Lett. **46**, 1275 (1981).

⁵H. J. Silverstone and P. M. Koch, J. Phys. B **12**, L537 (1979).

⁶P. M. Koch, J. Phys. (Paris) Colloq. **43**, C2-187 (1982).

⁷T. Bergeman, C. Harvey, K. B. Butterfield, H. C. Bryant, D. A. Clark, P. A. M. Gram, D. MacArthur, M. Davis, J. Dayton, and W. W. Smith (private communication).

⁸H. Rottke, H. Zacharias, and K. H. Welge, in *Laser Techniques for Extreme Ultraviolet Spectroscopy* (Boulder, 1982),

edited by T. J. McIlrath and R. R. Freeman (AIP, New York, 1982), pp. 402–421.

⁹K. H. Welge and H. Rottke, in *Laser Techniques in the Extreme Ultraviolet (OSA, Boulder, Colorado, 1984)*, edited by S. E. Harris and T. B. Lucatorto (AIP, New York, 1984), pp. 213–219; K. H. Welge and H. Rottke, in *Atomic Excitation and Recombination in External Fields*, edited by M. H. Nayfeh and C. Clark (Harwood Academic, New York, 1985); H. Rottke, A. Holle, and K. H. Welge, in *Fundamentals of Laser Interactions*, Vol. 229 of *Lecture Notes in Physics*, edited by F. Ehlotzky (Springer, Berlin, 1985).

¹⁰W. Glab and M. H. Nayfeh, Phys. Rev. A **31**, 530 (1985); W. Glab, K. Ng, D. Yao, and M. H. Nayfeh, *ibid.* **31**, 3677 (1985); M. H. Nayfeh *et al.*, in *Atomic Excitation and Recombination in External Fields*, edited by M. H. Nayfeh and C. Clark (Harwood Academic, New York, 1985).

¹¹H. A. Bethe and E. E. Salpeter, *Quantum Mechanics of One- and Two-Electron Atoms* (Springer, Berlin, 1957).

- ¹²R. J. Damburg and V. V. Kolosov, *J. Phys. B* **9**, 3149 (1976).
¹³E. Luc-Koenig and A. Bachelier, *J. Phys. B* **13**, 1743 (1980);
13, 1769 (1980).
¹⁴D. Farrelly and W. P. Reinhardt, *J. Phys. B* **16**, 2103 (1983).
¹⁵H. J. Silverstone, *Phys. Rev. A* **18**, 1853 (1978).
¹⁶H. J. Silverstone, B. G. Adams, J. Cizek, and P. Otto, *Phys. Rev. Lett.* **43**, 1498 (1979).
¹⁷R. J. Damburg and V. V. Kolosov, *J. Phys. B* **14**, 829 (1981).
¹⁸M. H. Rice and R. H. Good, Jr., *J. Opt. Soc. Am.* **52**, 239 (1962).
¹⁹G. F. Drukarev, *Zh. Eksp. Teor. Fiz.* **75**, 473 (1978) [*Sov. Phys.—JETP* **48**, 237 (1978)].
²⁰V. D. Kondratovich and V. N. Ostrovsky, *Zh. Eksp. Teor. Fiz.* **79**, 395 (1980) [*Sov. Phys.—JETP* **52**, 198 (1980)].
²¹D. A. Harmin, *Phys. Rev. A* **24**, 2491 (1981).
²²D. A. Harmin, *Phys. Rev. A* **26**, 2656 (1982).
²³V. D. Kondratovich and V. N. Ostrovsky, *J. Phys. B* **17**, 1981 (1984); **17**, 2011 (1984).
²⁴A. R. P. Rau and K. T. Lu, *Phys. Rev. A* **21**, 1057 (1980).
²⁵A. R. P. Rau, *J. Phys. B* **12**, L193 (1979).
²⁶R. R. Freeman, N. P. Economou, G. C. Bjorklund, and K. T. Lu, *Phys. Rev. Lett.* **41**, 1463 (1978).
²⁷R. R. Freeman and N. P. Economou, *Phys. Rev. A* **20**, 2356 (1979).
²⁸T. S. Luk, L. DiMauro, T. Bergeman, and H. Metcalf, *Phys. Rev. Lett.* **47**, 83 (1981).
²⁹W. Sandner, K. A. Safinya, and T. F. Gallagher, *Phys. Rev. A* **23**, 2448 (1981).
³⁰H. Zacharias, H. Rottke, J. Danon, and K. H. Welge, *Opt. Commun* **37**, 15 (1981).
³¹G. Lüders, *Ann. Phys. (Leipzig)* **8**, 301 (1951).
³²R. J. Damburg and V. V. Kolosov, *J. Phys. B* **12**, 2637 (1979).
³³G. A. Baker, Jr., *Essentials of Padé Approximants* (Academic, New York, 1975).
³⁴W. P. Reinhardt, *J. Phys. B* **16**, L635 (1983).